Multi-objective optimization of the management of a waterworks using an integrated well field model

Annette K. Hansen, Henrik Madsen, Peter Bauer-Gottwein, Anne Katrine V. Falk and Dan Rosbjerg

ABSTRACT

This study uses multi-objective optimization of an integrated well field model to improve the management of a waterworks. The well field model, called WELLNES (WELL field Numerical Engine Shell) is a dynamic coupling of a groundwater model, a pipe network model, and a well model. WELLNES is capable of predicting the water level and the energy consumption of the individual production wells. The model has been applied to Søndersø waterworks in Denmark, where it predicts the energy consumption within 1.8% of the observed. The objectives of the optimization problem are to minimize the specific energy of the waterworks and to avoid inflow of contaminated water from a nearby contaminated site. The decision variables are the pump status (on/off), and the constraint is that the waterworks has to provide a certain amount of drinking water. The advantage of multi-objective optimization is that the Pareto curve provides the decision-makers with compromise solutions between the two competing objectives. In the test case the Pareto optimal solutions are compared with an exhaustive benchmark solution. It is shown that the energy consumption can be reduced by 4% by changing the pumping configuration without violating the protection against contamination.

Key words | multi-objective optimization, PISA, pump energy consumption, water management, waterworks, well field

Annette K. Hansen (corresponding author)
Peter Bauer-Gottwein
Dan Rosbjerg
Department of Environmental Engineering,
Technical University of Denmark,
Miljoevej, Building 113,
DK-2800 Kongens Lyngby
Denmark
E-mail: *akha@env.dtu.dk*

Henrik Madsen
Anne Katrine V. Falk
DHI Water – Environment – Health,
Agern Allé 5,
DK-2970 Hørsholm,
Denmark

INTRODUCTION

In Denmark, 98% of the drinking water comes from groundwater. The amount of energy used to extract the water is considerable, and even a small reduction in the specific energy consumption (i.e. the energy in kWh per volume of pumped water) can result in a large overall reduction of energy consumption. Refsgaard *et al.* (2009) estimated that a reduction of 11% of the total annual energy consumption for groundwater pumping in Denmark is possible with improved pumping strategies. The Danish waterworks abstract about 392 million m^3 of groundwater per year (2006 data, Thorling 2009). With an average specific energy consumption of around $0.2 \, kWh/m^3$, an 11% reduction will result in a yearly saving of 8.6 GWh. During the last 15 years, on average 100 production wells in

Denmark have been closed per year due to contamination, often with pesticide or nitrate (Thorling 2009). This situation increases the pressure on the remaining production wells to fulfil the water demand. Moreover, it is difficult to find locations for new well fields in the densely populated area of Denmark. This paper presents a method to improve the management of existing waterworks with respect to the objectives of reducing energy consumption and preventing contamination of the wells.

Extensive research in optimal well field design and management has been performed (Mayer *et al.* 2002; Fowler *et al.* 2004). Using groundwater models, previous studies have, among other things, targeted optimal well positions or pumping rates. Similarly, numerous contributions have

addressed the optimal design of water distribution systems, for example optimal pumping rates, pipe sizing, and pipe lengths, using pipe network models (van Zyl *et al.* 2004; Farmani *et al.* 2005; Lopez-Ibanez *et al.* 2008). However, few studies have investigated the fully coupled hydrological and hydraulic system in a well field; including the flow of water in the aquifer, in the wells, and in the pipe network (Tsai *et al.* 2009). In this study a well field model called WELLNES is used to optimize the management of a waterworks (Madsen *et al.* 2009). WELLNES couples a groundwater model (Graham & Butts 2006), a well model (Halford & Hanson 2002; Konikow *et al.* 2009), and a pipe network model (Rossman 2000) and is capable of simulating the hydrological and hydraulic conditions in and around a well field. In addition, WELLNES includes an energy module that predicts the energy consumption of individuals pumps based on pump characteristic curves. Madsen *et al.* (2009) give a description of the WELLNES implementation.

Different methods to solve the highly non-linear problem of optimizing groundwater management have been investigated (Christensen & Hansen 1990; Fowler *et al.* 2008). Genetic algorithms emerge as one promising option. A review on genetic algorithms used in water resources planning and management has been published by Nicklow *et al.* (2010). If single-objective optimization is used, individual management objectives have to be aggregated into one objective function. This situation forces the decision-makers to decide on the relative importance of the objectives prior to the optimization without full knowledge about the trade-offs between objectives. Different objectives can be conflicting; thus, improving one objective will reduce the performance with respect to other objectives. Using multi-objective optimization, the whole set of non-dominated solutions (Pareto optimal set) is found (Kollat & Reed 2006; Siegfried & Kinzelbach 2006; Siegfried *et al.* 2009) and the decision-makers can subsequently choose a preferred solution among the Pareto optimal solutions using other types of information not directly included in the optimization.

This paper presents an approach to improve the management of a waterworks using multi-objective optimization. The objectives are to minimize the energy consumption and to minimize the risk of well field contamination from a nearby contaminated site, subject to the constraint of providing a certain amount of drinking water. We use a medium-sized Danish waterworks, Søndersø waterworks, as case study. The waterworks is located northwest of Copenhagen, Denmark. The aquifer system and the raw water pipe network have been implemented in the WELLNES model. In the following a description of the WELLNES model is given, followed by a description of the optimization algorithm. Subsequently the results are presented, followed by a discussion and conclusions.

MODEL DESCRIPTION

WELLNES was developed for integrated simulations of the hydrological and hydraulic conditions in and around a well field. WELLNES is a shell program, developed by DHI that facilitates a dynamic coupling between a groundwater model and a pipe network model (Madsen *et al.* 2009; Refsgaard *et al.* 2009). It simulates the water flow in the well field and in the pipe network. The coupling of the groundwater model and the pipe network model ensures consistent pressure distribution and flow rates across the compartments. The shell program uses the Open Modeling Interface, OpenMI (Gregersen *et al.* 2007), which allows different models to be plugged into the shell. In this study the groundwater model is the MIKE SHE model (Graham & Butts 2006) and the pipe network model is the EPANET model (Rossman 2000).

The steep hydraulic gradient close to a production well is not accurately represented in a finite-difference groundwater model if the radius of the cone of depression is much smaller than the horizontal dimension of the numerical grid cell. There is a significant difference between the average head simulated in the numerical grid cell and the head in the pumping well (cell-to-well head loss). Moreover, there can be significant head losses across the screens of the wells (well head loss). Both effects cause the actual water level in the well to be lower than the water level predicted by the groundwater model. To account for this the groundwater model is coupled with a well model based on the same equations as the Multi Node Well module of MODFLOW (Halford & Hanson 2002; Konikow *et al.* 2009). If the well is screened over n vertical numerical cells, the

total pumping rate Q [L^3/T] from the well is:

$$Q = Q_1 + Q_2 + \cdots + Q_i + \cdots + Q_n, \qquad (1)$$

where Q_i [L^3/T] is the pumping rate from the ith cell.

The difference between the head in the cell, h_i [L], and the head in the well, h_{well} [L], can be described with a general well-loss equation:

$$h_{\text{well}} - h_i = AQ_i + BQ_i + CQ_i^P \qquad (2)$$

where A is a linear aquifer-loss coefficient [T/L^2], B is a linear well-loss coefficient [T/L^2], C is a nonlinear well-loss coefficient [T^P/L^{3P-1}], and P is the power of the nonlinear discharge component of well loss. In case of abstraction Q is negative.

The cell-to-well head-loss term, AQ_i, is caused by the well having a radius less than the horizontal dimensions of the cell, hence in case of abstraction the head in the well is lower than the head in the cell. If terms B and C are negligible, the head-loss can be calculated by using the Thiem steady-state flow equation and Equation (2) becomes:

$$h_{\text{well}} = h_i + \frac{Q_i}{2\pi T} \ln \frac{r_0}{r_{\text{w}}}, \qquad (3)$$

where T [L^2/T] is the transmissivity of the aquifer, and r_{w} [L] is the actual radius of the well. The effective radius of the finite-difference cell, r_0 [L], is equivalent to the radius of a vertical pumping well, which would have the same head as the head calculated for the node of the cell. For isotropic porous media $r_0 = 0.14\sqrt{\Delta x^2 + \Delta y^2}$, where Δx and Δy are the grid spacing. The constant term $(1/2\pi T) \ln (r_0/r_{\text{w}})$ is the cell-to-head-loss coefficient, A.

The linear well-loss coefficient, B, in Equation (2) defines the well head losses from flow through formation damaged during well drilling, gravel pack, and the well screen. The area of the affected formation is called the skin. B can be reformulated into a skin factor (Halford & Hanson 2002)

$$\text{skin} = \left(\frac{K_h b}{K_{\text{skin}} b_{\text{w}}} - 1 \right) \ln \left(\frac{r_{\text{skin}}}{r_{\text{w}}} \right), \qquad (4)$$

where b [L] is the saturated thickness of the cell, b_{w} [L] is the saturated length of the borehole in the cell ($b_{\text{w}} = b$ for a fully

penetrating vertical well), K_{skin} [L/T] is the hydraulic conductivity of the skin, K_h [L/T] is the effective horizontal hydraulic conductivity of the cell, and r_{skin} [L] is the radius of the skin. When anisotropy is present $K_h = \sqrt{K_x K_y}$. The relation between the skin factor and B is given by:

$$B = \frac{\text{skin}}{2\pi b \sqrt{K_x K_y}}. \qquad (5)$$

If the hydraulic conductivity of the skin is smaller than the hydraulic conductivity of the cell ($K_{\text{skin}} < K_h$), then the skin and B become positive. In case of abstraction (Q negative) the contribution to Equation (2) becomes negative giving a water level in the well that is lower than in the cell. The term CQ_i^P in Equation (2) is the non-linear well loss caused by any turbulent flow near the well (Konikow *et al.* 2009).

The coupling between the groundwater model, the pipe network model and the well model is not straight forward. In the coupling of the models the pumping rate is a boundary condition to the groundwater model, and the water level of the well is a boundary condition to the pipe network model. In each time step iteration is performed between the groundwater model and the pipe network model via the well model to obtain the water level and the pumping rate in the well. In the WELLNES model each pumping well introduces an additional calibration parameter, the skin factor.

An energy module calculates the energy consumption of the pumps. The energy module uses pump curves (relationships between power, pumping rate and dynamic head, P-Q-h_{dyn}-curves) to calculate the energy consumptions. The manufacturer provides a unique set of pump curves for each pump type. An example of a set of pump curves for an on/off pump can be seen as the bold solid line in Figure 1. The lower panel of Figure 1 shows the connection between the pumping rate, Q, and the power, P. If for example the total dynamic head, h_{dyn}, is 35 m, the pump will deliver 80 m^3/h and the pump will use 10 kW. If the total dynamic head is 42 m, the pump will only deliver 65 m^3/h, but use 10.8 kW. Typically, the power consumption of these types of pumps does not vary more than a few kW along the range of Q. This means that the variations in energy consumption of the pumps are smaller than the variations in pumping rates. Therefore, the specific energy
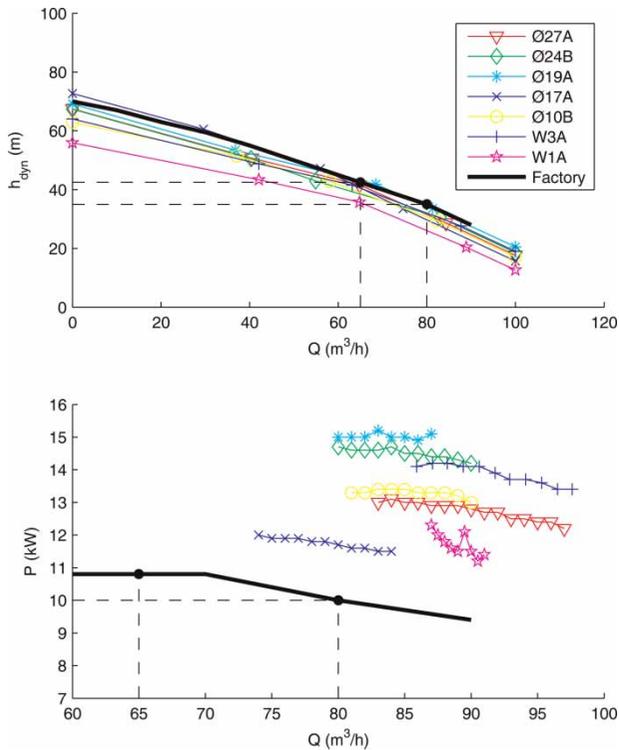
Figure 1 | P-Q-h_{dyn}-curves of the SP75-4 pump at Søndersø waterworks. P is power [kW], Q is pumping rate [m³/h], and h_{dyn} is the total dynamic head [m]. The pump type is situated in well Ø27A, Ø24B, Ø19A, Ø17A, Ø10B, V3A, and V1A.

consumption varies considerably over the range of feasible dynamic heads.

The pump curves change over time due to wear and clogging of the pumps. The effective pump curves are obtained by measuring water level, pumping rate and power for different pumping operations. In WELLNES the Q-h_{dyn}-curves are included in the pipe network model, and the Q-P-curves in the energy module.

Case study: Søndersø waterworks

Area

The WELLNES model was implemented and used for multi-objective optimization at the Søndersø waterworks, a medium size Danish waterworks, which extracts around 20,000 m³ of water per day. The waterworks consists of three well fields (Figure 2); Søndersø East with eight submersible pumps, Søndersø West with three submersible pumps, and Tibberup with 10 wells connected to a siphon

system with a vacuum tank. Søndersø East and West are located along the shore of Lake Søndersø, whereas Tibberup is located along Tibberup stream.

The now closed Værløse air field is located, west of Søndersø waterworks. which is known to be contaminated with chlorinated hydrocarbon compounds. Several protective wells have been installed both in the secondary and primary aquifers, from where the water is pumped, treated and finally discharged into the local Jonstrup stream. The concern is to prevent the contaminated water flowing from the air field towards the well field and thereby contaminating the drinking water wells.

The primary aquifer in the area is the Tertiary Danian limestone, located approximately 30 m below mean sea level in most of the domain, but rising to mean sea level towards the north. The thickness of this layer is approximately 25 m. Above the limestone lies an undulating glaciomorphological topography consisting of shifting irregular layers of Quaternary clayey and sandy deposits. One larger sand layer exists in the area in which one well (Ø20A) is screened. The thickness of the sand layer varies from almost 0 in the southwestern part of the area to a thickness of 45 m in the northern and northeastern part. There is no direct hydraulic connection between Lake Søndersø and the aquifer.

Model set-up and calibration

The MIKE SHE model (Graham & Butts 2006) was used to simulate the groundwater flow system in the Søndersø area. The model is a local finite-difference model nested into an existing regional groundwater model. The regional model is a fully distributed and integrated hydrologic model covering Zealand, established by the Environment Center Roskilde (Kürstein et al. 2009).

The local Søndersø model covers an area of approximately 7×4 km, and the grid size is 50×50 m. The geological representation of the regional model's saturated zone was used directly with minor modification. Five of the regional model's 13 geological layers were not present within the local model domain. An east–west and a north–south cross section of the geological model can be seen in Figures 3 and 4.

Recharge to the saturated zone simulated by the regional model was used as groundwater recharge in the
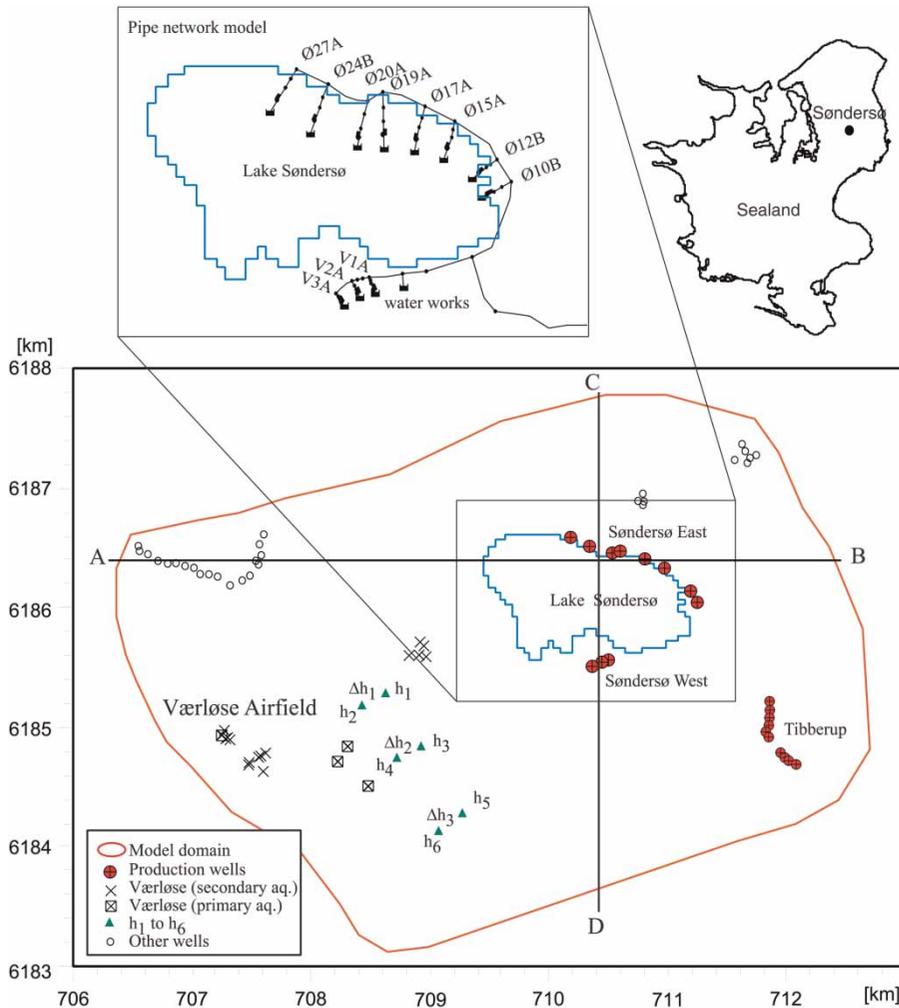
Figure 2 | Sketch of the Søndersø area and model domain. Cross-section along line AB and BC can be seen in Figures 3 and 4.
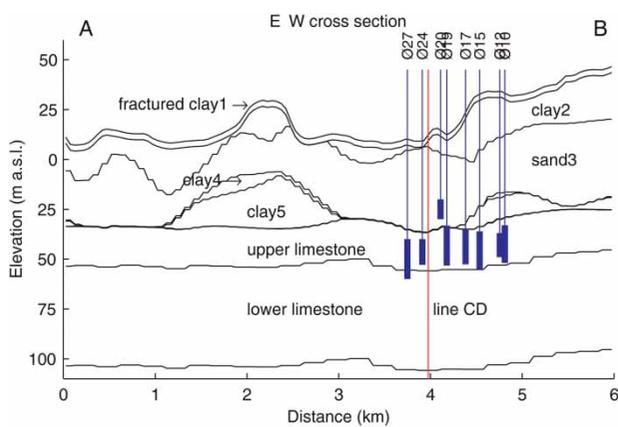

Figure 3 | Cross-section along the line AB in Figure 2. Well positions and filter depth are shown, as well as the crossing of line CD.
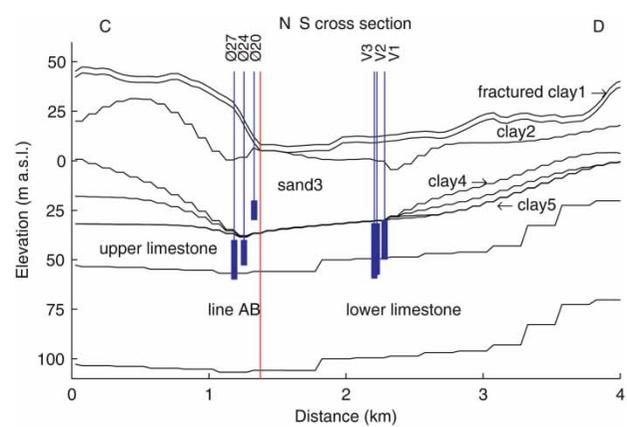
Figure 4 | Cross-section along the line CD in Figure 2. Well positions and filter depth are shown, as well as the crossing of line AB.

local model. The regional model uses gridded climate data of precipitation, air temperature and evapotranspiration provided by the Danish Meteorological Institute. Simulated heads produced by the regional model are used as Dirichlet boundary conditions in the nested local model.

A clay lens is represented at the interface between the clay5 layer and the upper limestone. The horizontal extension of the lens is a 1 km wide band covering the lake and approximately 2 km towards both the west and east of the lake and its thickness is between 2 and 7 m. The Søndersø East wells are located within this lens area but Søndersø West and Tibberup are not. During the calibration it became clear that the lens was essential for describing a difference in hydrogeology between Søndersø East and West with different dynamic behaviour when the pumps were turned on and off.

In the process of setting up and calibrating the model we found that the regional model under-estimated groundwater recharge in the Søndersø area. The head values in the primary aquifer around Lake Søndersø were decreasing steadily during the evaluation period of 10 years, while observed piezometric heads were stable over the same period. Groundwater recharge in the regional model was therefore increased by 40%, which resulted in a satisfactory match of simulated and observed groundwater heads.

All known wells within the domain were included in the model and can be seen in Figure 2. The relevant wells for this study are the 11 abstraction wells at Søndersø West and Søndersø East and the 19 protection wells at Værløse air field. One of the 11 abstraction wells (Ø20A) is screened in the sand aquifer (sand3), and the rest are screened in the limestone aquifer. Four of the 19 wells at the air field are screened in the limestone aquifer, and the rest in the sand aquifer (sand3).

The purpose of this study is to improve the management of Søndersø waterworks. It is essential that the model accurately predicts the groundwater level response to pump scheduling. In the period from 3 November 2008 to 15 July 2009 multiple pump tests were performed. The first test period extends from 3 November 2008 to 8 April 2009; the second period from 25 April 2009 to 15 July 2009. Hourly data of head, pumping rate and energy consumption were recorded in the waterworks' SCADA system. This exceptional dataset was used to refine the local model. The first period was used for calibration, and the second period for validation. The local model is hot-started using a long-time simulation from 2000 with initial conditions taken from the regional model and runs with an hourly time step.

In the calibration of the groundwater model, priority was given to an accurate reproduction of the static groundwater level during periods when the pump is off. We accept a (preferably positive) bias when the pump is on, as the well model will account for the difference between the head in the groundwater numerical cell and the head in the well.

After calibration of the groundwater model, the model was coupled to the well model in WELLNES. The well model needs calibration of the skin factor to correctly simulate well drawdown when the pumps are on. Each well was calibrated successively by trial-and-error. Finally, the pipe network model for Søndersø waterworks was set up and calibrated and coupled to WELLNES. The calibration parameters here are the roughness coefficients of the pipes.

In the present version of the WELLNES set-up for Søndersø, the Tibberup siphon system is not coupled to the WELLNES model. Instead, the Tibberup well field is included in the groundwater model. The measured abstraction rate is divided between the wells according to key figures from flow measurements. The water from Tibberup enters the pipe network model as a forcing at the junction point.

Performance of model

Figures 5–7 show the observed and simulated head elevation for three selected wells, Ø24A, Ø10B and V2A. Both the calibration period and the validation period are shown. The model accurately simulates the water level dynamics when the pumps are turned on and off, and it predicts the overall head elevation level satisfactorily, both when pumps are on (low level) and off (high level). The model generally underestimates the water level in V3A, but it is able to simulate the amplitude of the variations. Also, at the two other wells at Søndersø West, the model underestimates the water level. Part of Figure 6 is enlarged in Figure 8. Overall model performance is
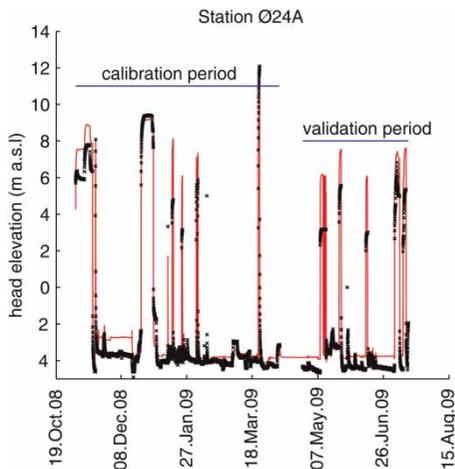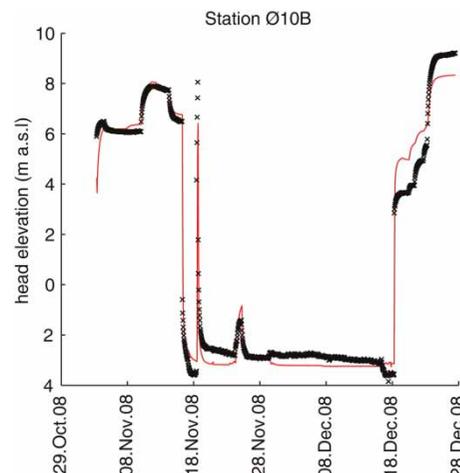
Figure 5 | Observation (crosses) and simulation (solid line) of head elevation head elevation in well Ø24B in both calibration and validation period.
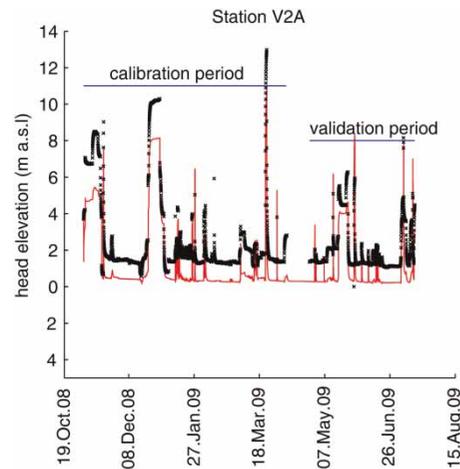
Figure 7 | Observation (crosses) and simulation (solid line) of head elevation in well V2A in both calibration and validation period.
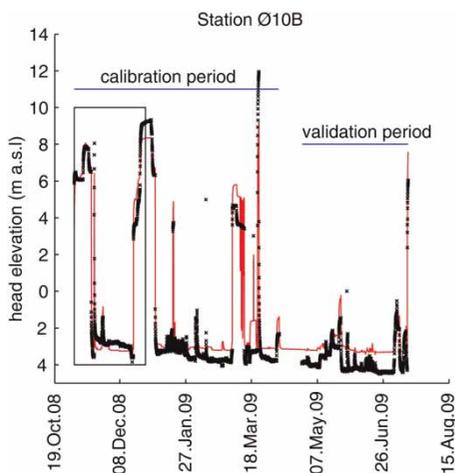
Figure 6 | Observation (crosses) and simulation (solid line) of head elevation in well Ø10B in both calibration and validation period. The rectangle illustrates the area which can be seen in Figure 8.
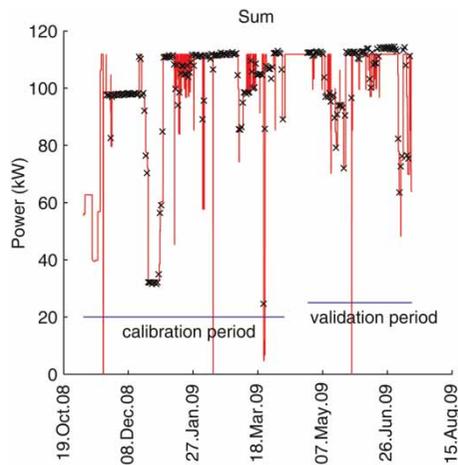

Figure 8 | Observation (crosses) and simulation (solid line) of head elevation in well Ø10B in both calibration and validation period. Enlargement of the rectangle shown in Figure 6.

satisfactory. At the start of the simulation, on 3 November, pump Ø10B along with three other pumps (Ø24B, Ø19A, V3A) is off. On 10 November, three additional pumps (Ø20A, Ø17A, Ø15A) are turned off, which gives rise to an increase in head. On 14 November two pumps (Ø20A, Ø17A) are switched on, resulting in a minor decrease in head just before all pumps are started on 15 November where the water level decreases by 10 m. The large peak on 18 November is due to all the pumps being turned off for one day. At the end of the period from 18 December onwards the pumps are successively turned off again, starting with Ø10B. Head variations due

to changes in the pump status are well predicted by the model. Figure 9 shows the total observed and simulated power consumption during the calibration and validation period; good correspondence is found.

Accumulated abstraction results for each well field are shown in Table 1. Results from both the calibration and validation period are shown. The model underestimates the total abstraction for both Søndersø West and East, performing slightly better for Søndersø East than Søndersø West. Table 2 shows the results for the accumulated energy consumption. Here the model predicts larger energy

Figure 9 | Observation (crosses) and simulation (solid line) of the total power consumption for Søndersø east and west in both calibration and validation period.

consumption than observed, except at Søndersø West in the validation period. The relative discrepancy is smaller than for the abstraction. This change is because the power curves are flat in the operational interval and an error in the pump rate will give a smaller error in the power consumption. In Søndersø the same pump type, SP75-4 is

placed in seven of the 11 wells. The effective pump curves for these seven wells are shown in Figure 1. The Q-h_{dyn}-curves are fairly close to the factory curves. The discrepancy between the factory and the effective P-Q-curve are larger than for the Q-h_{dyn}-curves, and the seven effective curves also differ significantly from each other. All pumps use more power than the factory curve indicates.

Multi-objective optimization

General description

Consider a well field consisting of n pumps which can be either on or off. The status of the pump, s_i, is set at the beginning of the model evaluation and is constant during the model evaluation. A pumping configuration (i.e. an individual in the evolutionary algorithm) can then be described by a binary string of length n (0 if the pump is off, 1 if the pump is on). For example, an individual could be $[s_1 s_2 s_3 \ldots s_i \ldots s_{n-1} s_n] = [100\ldots1\ldots10]$.

WELLNES provides the pumping rates, $Q_i(t)$ [m³/h], and the power consumption, $P_i(t)$ [kW], for the ith well at

Table 1 | Observed and simulated abstraction in m³ for the calibration period 1, and the validation period 2, and the absolute and relative discrepancies between simulated and observed data

	Period 1			Period 2		
	East	West	Tib	East	West	Tib
Obs [m³]	1,676,592	743,668	959,664	952,158	401,215	580,290
% of total extrac.	49.6%	22.0%	28.4%	49.2%	20.7%	30.0%
Sim [m³]	1,624,026	705,462	Not sim	921,752	375,457	Not sim
Sim-Obs, abs [m³]	−52,566	−38,206	Not sim	−30,406	−25,758	Not sim
Sim-Obs, rel	−3.1%	−5.1%	Not sim	−3.2%	−6.4%	Not sim

Table 2 | Observed and simulated energy consumption in kWh for the calibration period 1, and the validation period 2, and the absolute and relative discrepancies between simulated and observed data

	Period 1			Period 2		
	East	West	Tib	East	West	Tib
Obs [kWh]	243,031	78,960	58,577	152,045	49,827	43,765
% of total extrac.	63.9%	20.8%	15.4%	61.9%	20.3%	17.8%
Sim [kWh]	243,896	80,366	Not sim	152,744	48,402	Not sim
Sim-Obs, abs [kWh]	865	14,106	Not sim	699	−1,425	Not sim
Sim-Obs, rel	0.4%	1.8%	Not sim	0.5%	−2.9%	Not sim

time t. The specific energy consumption of the waterworks as function of time, $e_{spe}(t)$ [kWh/m^3], is given by:

$$e_{spe}(t) = \frac{\sum_{i=n}^{n} P_i(t)}{\sum_{i=n}^{n} Q_i(t)} \tag{6}$$

The average of the specific energy in the evaluation period is $E_{spe} = \overline{e_{spe}(t)}$.

Groundwater in an area close to the well field is contaminated. It is of interest to keep this contamination away from the well field. Several methods exist to transform the contamination problem into a measurable value that can be used in the optimization framework. One method is to use head values, $h_i(t)$, at selected locations between the contaminated site and the well field. The pair wise differences in the observations, $\Delta h_i(t)$, give the direction of the flow, and a positive value indicates a flow away from the well field. $H = \overline{h_i(t)}$ is the mean of the i pairs of $\Delta h_i(t)$ in the evaluation period. As the objective is to keep the contaminated water away from the well field, it is desirable to have an H value as large as possible.

In this two-dimensional optimization problem the objectives are to minimise the specific energy, E_{spe}, and to maximize the head differences, H, subject to the constraint of fulfilling a demand of water abstraction, Q_{dem} [m^3/h]. The optimization problem can be written as:

$$\begin{aligned} \min \quad & E_{spe} \\ \max \quad & H \\ \text{s.t.} \quad & Q_{tot} \geq Q_{dem} \end{aligned} \tag{7}$$

Q_{tot} is the total amount of abstracted water from the well field.

Genetic algorithm

A genetic algorithm is used to solve the multi-objective optimization problem. The genetic algorithm works with a population of individuals, where an individual is one set of pumping configurations for the waterworks. The evolution proceeds in generations, and the population for the first generation (size α) is generated randomly. In each generation, selection and recombination is performed. In the selection the best λ individuals are, based on the objective

function values, chosen and transferred to a mating pool. In the mating pool the individuals are recombined by crossover and mutation. Crossover uses the existing individuals to create new and better individuals. Mutation introduces new genes into the population. In each generation a WELLNES model simulation is performed for each individual in the mating pool that has not already been evaluated. From these simulations objective functions are calculated. All individuals and their objective function values are saved in an archive. Before simulating the WELLNES model the archive is searched for a previously identical simulation. If a match is found the objective function values are taken from the archive. This results in a large reduction in CPU time. The algorithm continues until a maximum number of generations is reached, and the optimization has converged to a set of optimal non-inferior pumping configurations.

The software PISA developed at ETH Zurich (Bleuler *et al.* 2003) is used to implement the genetic algorithm. The software divides the optimization problem into a problem independent part (the selector) and a problem dependent part (the variator). The only necessary exchange of information between the variator and the selector are the individual IDs (corresponding to individual pumping configuration) and their objective function values.

The selector handles the procedure of selecting the individuals to be transferred to the mating pool and PISA provides different selector modules that are coupled with the user's optimization problem. The Strength Pareto Evolutionary Algorithm 2 selector algorithm (SPEA2) is implemented in this optimization problem (Zitzler *et al.* 2002).

The variator controls the evolution of the genetic algorithm, and it handles the evaluation of the model (link to the WELLNES model), recombination, constraint handling, communication to the selector and archiving. The coding of the variator is performed in Matlab. Single-point crossover and bit-wise mutation (with mutation rate p_μ) are used for recombination of individuals (Deb 2001). If an individual violates the constraint, its objective values will be set to a value larger than any feasible solution. During the next generation, this individual will be excluded from the population by the selector.

Søndersø waterworks

Søndersø waterworks has 11 pumps and the connection between an individual and the pumping configuration is as follows (Figure 2): $[s_1 s_2 s_3 \ldots s_i \ldots s_{10} s_{11}] = $ [Ø27A, Ø24B, Ø20A, Ø17A, Ø15A, Ø12B, Ø10B, V3A, V2A, V1A]. The contaminated site, Værløse air field, is located west-south-west of the waterworks. Particle tracking is used to find the water divide between the well field and the air field. Three pairs of head differences, Δh_1, Δh_2 and Δh_3, are in the groundwater model placed along the water divide (Figure 2) for calculation of the objective function H. The demand of water the waterworks has to provide is $Q_{\text{dem}} = 454 \, \text{m}^3/\text{h}$, which is the observed abstraction in the simulation period. The optimization is performed using WELLNES simulating the period from 3 November 2008 to 10 November 2008. In the optimization algorithm values of $\alpha = 100$, $\lambda = [16, 20, 26]$ and $p_\mu = 0.2$ are used. The maximum number of generations is 80.

RESULTS

Figure 10 shows the Pareto optimal set of solutions and their respective pumping configurations. Three different values of λ are shown ($\lambda = [16, 20, 26]$). The number of model evaluations, N, for these three solutions is shown in Table 3. The number of model evaluations required if no archiving was used is also shown. The benchmark solution to the optimization problem has been calculated by simulating all 2^{11} different pumping configurations. The benchmark solution is shown in Figure 11. The Pareto front forms a

Table 3 │ N is number of model evaluation, N(noArc) is number of model evaluation in case of no archiving, HV is the hypervolume indicator

λ	N	N(noArc)	HV
16	185	1,380	0.98
20	199	1,700	0.85
26	193	2,180	0.99
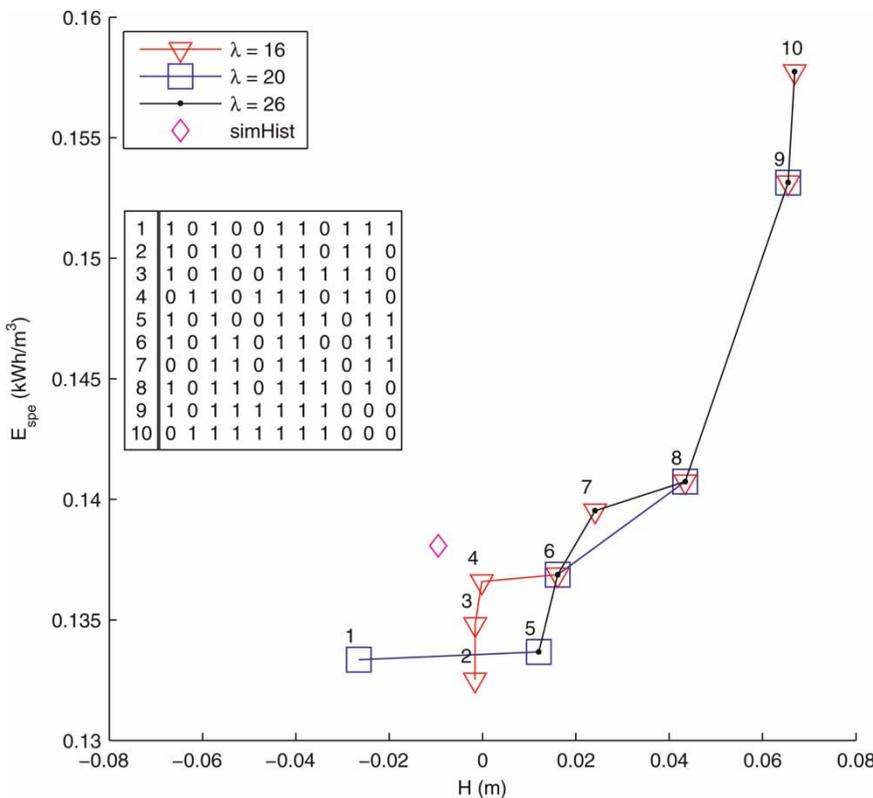
Figure 10 │ Pareto front for three optimization runs with $\lambda = 16$ (triangle), $\lambda = 20$ (squares), and $\lambda = 26$ (black dots). The pumping configurations for the numbered solutions are shown in the box. The diamond is the objective values of the simulated history.
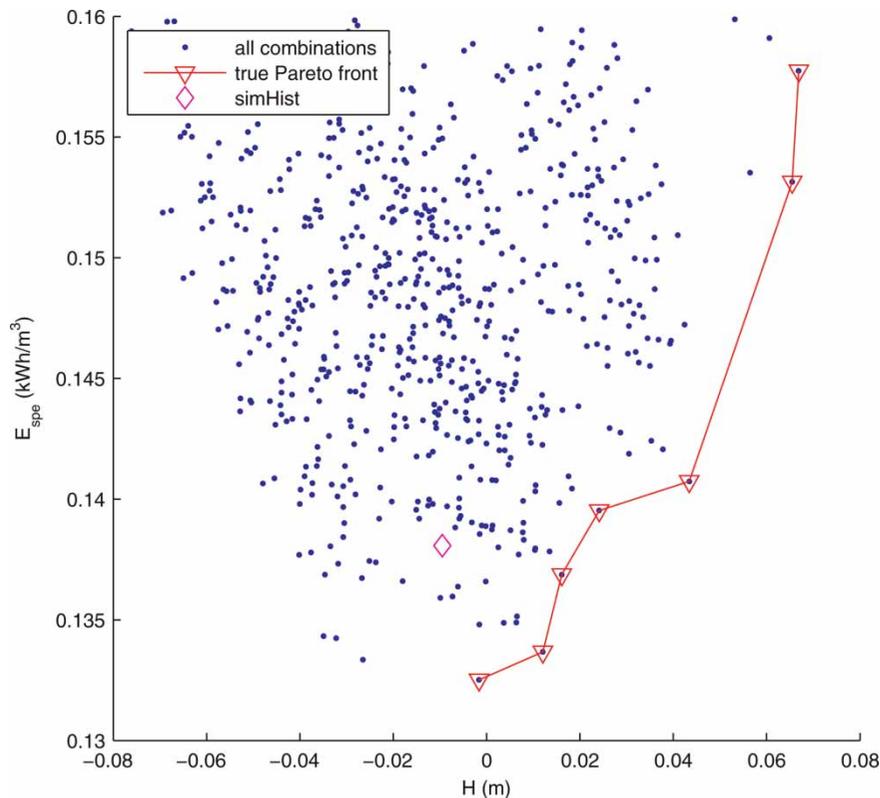
Figure 11 │ Benchmark solution. The solid line is the true Pareto front. The dots are all 2^{11} different pumping configurations. The diamond is the simulated history solution.

predominantly convex trade-off curve between the two objectives, minimizing E_{spe} and maximizing H. For H values between 0.01 and 0.05, the Pareto curve has a concave area. All optimization scenarios show good convergence to the true Pareto front, but minor dissimilarities occur in the concave area. The hypervolume indicator (HV) (Knowles *et al.* 2006) for the three scenarios is shown in Table 3. The closer HV is to one, the closer is the front to the true Pareto front. The scenarios with λ equal to 16 and 26 are closest to the benchmark solution, and they are also the most effective with respect to number of model evaluations. However, all three scenarios are both effective and efficient. The archiving reduces the CPU time dramatically.

There are 10 unique solutions in the plot in Figure 10. The mean pumping rates for each solution are presented in Table 4, the mean power consumption per time step in Table 5, and the mean specific energy in Table 6. When a pump is on, the $\bar{Q}_i$, $\bar{P}_i$ and $\bar{e}_{spe,i}$-values vary slightly depending on the status of the neighbouring pumps. For example, the pumping rate of well Ø15A varies between 32.13 and 34.80 m^3/day for the 10 different solutions shown in Table 4. This number supports the results from Figure 8, where the water level in well Ø10B changes when the other wells are turned on and off.

Søndersø West has a great impact on the objective function values. The pumps at Søndersø West have low e_{spe}, especially $e_{spe}(V2A) \approx 0.09(\text{kWh/m}^3)$, which gives an overall low E_{spe} when two or more pumps at Søndersø West are on (solutions 1–7). However, as Søndersø West is close to Værløse air field, the pumps here also have a large negative impact on the second objective value, H. Solutions 9 and 10 have all three pumps at Søndersø West off, which result in the highest possible H value.

It is interesting to note the difference between solution 9 and 10. Solution 10 uses 19% more energy than solution 9, and provides an increase of 0.07 m in H. The two solutions have almost identical pumping configurations. The only difference is the pumping at Ø27A and Ø24B, where solution 9 has pump Ø27A on and pump Ø24B off. Solution

Table 4 | Mean pumping rates $\bar{Q}_i$ [m³/h] for each well for different pumping configurations. IDnr refers to the solution number shown in Figure 10

$\bar{Q}_i$ [m³/h]

IDnr	Ø27A	Ø24B	Ø20A	Ø19A	Ø17A	Ø15A	Ø12B	Ø10B	V3A	V2A	V1A	$\sum \bar{Q}_i$
1	90.45	0	40.05	0	0	34.80	63.34	0	91.55	57.26	84.36	461.80
2	88.94	0	39.46	0	81.40	33.61	62.44	0	93.30	60.40	0	459.55
3	89.87	0	39.78	0	0	34.13	61.21	85.57	93.22	60.29	0	464.08
4	0	86.88	39.48	0	81.19	33.54	62.38	0	93.28	60.35	0	457.09
5	89.88	0	39.79	0	0	34.10	61.17	85.52	0	60.95	86.32	457.74
6	88.79	0	39.00	85.99	0	34.22	62.87	0	0	61.22	86.61	458.69
7	0	0	39.52	87.07	0	34.08	61.18	85.54	0	61.08	86.44	454.90
8	88.16	0	38.74	85.27	0	33.52	60.71	85.03	0	64.42	0	455.85
9	86.25	0	38.10	83.15	78.04	32.19	59.64	83.79	0	0	0	461.17
10	0	84.04	38.12	83.02	77.86	32.13	59.59	83.73	0	0	0	458.50

Table 5 | Mean power consumption $\bar{P}_i$ [kW] for each well for different pumping configurations. IDnr refers to the solution number shown in Figure 10

$\bar{P}_i$ [kW]

IDnr	Ø27A	Ø24B	Ø20A	Ø19A	Ø17A	Ø15A	Ø12B	Ø10B	V3A	V2A	V1A	$\sum \bar{P}_i$
1	12.753	0	4.800	0	0	5.501	6.805	0	13.939	5.501	12.298	61.60
2	12.890	0	4.800	0	11.606	5.537	6.852	0	13.705	5.523	0	60.91
3	12.808	0	4.800	0	0	5.504	6.904	13.337	13.706	5.518	0	62.58
4	0	14.416	4.800	0	11.608	5.544	6.858	0	13.705	5.521	0	62.45
5	12.807	0	4.800	0	0	5.504	6.905	13.342	0	5.549	12.298	61.20
6	12.895	0	4.800	14.926	0	5.503	6.817	0	0	5.562	12.297	62.80
7	0	0	4.800	15.091	0	5.504	6.905	13.340	0	5.555	12.298	63.49
8	12.900	0	4.800	14.971	0	5.545	6.928	13.381	0	5.650	0	64.18
9	12.969	0	4.800	15.157	11.807	5.523	6.999	13.395	0	0	0	70.65
10	0	14.660	4.800	15.168	11.817	5.519	6.999	13.395	0	0	0	72.35

Table 6 | Mean specific energy consumption $\bar{e}_{\text{spe},i} = (P_i/Q_i)$ [kWh/m³] for each well for different pumping configurations. $E_{\text{spe}} = \sum P_i / \sum Q_i$ is the specific energy consumption for the water works. The IDnr refers to the solution numbers shown in Figure 10

$\bar{e}_{\text{spe},i}$ [kWh/m³]

IDnr	Ø27A	Ø24B	Ø20A	Ø19A	Ø17A	Ø15A	Ø12B	Ø10B	V3A	V2A	V1A	e_{spe}
1	0.141	0	0.120	0	0	0.158	0.107	0	0.152	0.096	0.146	0.133
2	0.145	0	0.122	0	0.143	0.165	0.110	0	0.147	0.091	0	0.133
3	0.143	0	0.121	0	0	0.161	0.113	0.156	0.147	0.092	0	0.135
4	0	0.166	0.122	0	0.143	0.165	0.110	0	0.147	0.092	0	0.137
5	0.143	0	0.121	0	0	0.161	0.113	0.156	0	0.091	0.142	0.134
6	0.145	0	0.123	0.174	0	0.161	0.108	0	0	0.091	0.142	0.137
7	0	0	0.122	0.173	0	0.161	0.113	0.156	0	0.091	0.142	0.140
8	0.146	0	0.124	0.175	0	0.165	0.114	0.157	0	0.088	0	0.141
9	0.150	0	0.126	0.182	0.151	0.171	0.117	0.160	0	0	0	0.153
10	0	0.174	0.126	0.183	0.152	0.172	0.117	0.160	0	0	0	0.158

10 is opposite. The pump types, the well depths, screens and hydraulic parameters for both wells are the same, but the pump in well Ø27A (e_{spe}(Ø27A) ≈ 0.14 kWh/m³) is more effective than the one in well Ø24B (e_{spe}(Ø24B) ≈ 0.17 kWh/m³). The slightly better H value in solution 10 shows that the operation at Søndersø East also has a minor impact on the gradient towards the contaminated Værløse air field.

The objective function values for WELLNES simulated with the historical pumping configuration are plotted as the diamond in Figure 10. For this specific period (3 November 2008 to 10 November 2008) it is possible to save 0.006 kWh/m³ or 4% of the energy consumption and obtain a slightly better protection against contamination (larger H value) if solution 2 is chosen.

DISCUSSION

The performance of WELLNES is good in general. The model performs better at Søndersø East than at Søndersø West. Both the error on the total abstraction and the error on the total energy consumption are larger for Søndersø West than for Søndersø East (Tables 1 and 2). The difference between the two well fields is also seen in the prediction of the water levels, where the water levels in all three wells at Søndersø West are approximately 1 m lower than the observed. The lens located right above the primary aquifer in the area of Søndersø East does not exist in the area of Søndersø West. Perhaps the horizontal extension of the lens and the stratigraphy below Søndersø West are not completely correct. If further work is to be performed on the calibration on the groundwater model, a closer investigation on the stratigraphy around Søndersø West should be carried out.

The high resolution data recorded by the waterworks SCADA system give a unique chance to observe the rapid change in heads, when pumps are turned on and off. The data show a large interaction between the wells. The water level in a well is affected when a well more than 1 km away is turned on or off. This finding demonstrates the need for an integrated modelling approach as implemented in WELLNES.

WELLNES has proven to be a useful tool in simulating the hydrology and hydraulics in the well field and to predict the energy consumption of the pumps, hence it is suitable to use in the optimization of the management. One limitation of the use of the model for optimization is that a high resolution of the groundwater model is usually required for simulating the dynamics of the well field accurately. A high-resolution groundwater model is CPU intensive, and the simulation of the groundwater model is by far the most CPU consuming part of the optimization. The task of calibrating a groundwater model that is able to simulate the dynamics of the well field is not trivial. It needs high resolution data which are typically not available in existing well databases.

The multi-objective optimization performs well; all three scenarios with $λ = 16, 20, 26$ are close to the benchmark solution, and the HV values for the scenarios are between 0.85 and 0.99. The optimization uses between 185 and 199 model evaluations to converge (Table 3), which is about 10% of the 2^{11} possible configurations. The scenario with $λ = 20$ fails to find solution 10, which has a large impact on HV, and the scenario also uses more model evaluations than the others. Both features can be ascribed to the random nature of the genetic algorithm.

It is interesting to study the results from the individual pumping configurations. Some pumps have low specific energy (Ø27A, Ø20A, Ø12B and V2A) and others high specific energy (Ø24B, Ø19A, Ø15A). In general, the most effective pumps are used when the objective values E_{spe} and H are low, and the most ineffective pumps are used when E_{spe} and H are high. It is interesting to note that seven pumps should be activated to fulfil the water demand in all 10 solutions.

In period 1, Søndersø waterworks operates with 86% of the pumps being on all the time. As the waterworks are operating so close to maximal capacity, the potential for saving energy by only changing the pumping configuration is small. Other possibilities for additional savings could be to install frequency regulators on all the pumps. This would increase the flexibility of the waterworks, but it will also make optimization of the waterworks more important, as calculation of a benchmark solution will be infeasible.

A future scenario could be to expand the waterworks capacity by replacing the pumps with newer and more effective pumps and investigate what the outcome would be for the energy consumption and the risk of contaminating into

the drinking water. This factor would give the waterworks increased flexibility when optimizing the pumping configuration, and, in addition, add a buffer capacity to the waterworks, both with respect to short time (breakdown at other waterworks) and long time increases in demand.

Multi-objective optimization is a useful tool for the decision-makers. In this case the operators at the waterworks can use the method for choosing the configuration of the pumps. Instead of choosing between the 2^{11} different possibly pumping configurations, they can choose between the seven optimal solutions on the Pareto front. To select a preferred solution they can use additional information not directly included in the optimization, such as considerations of wear and clogging of the pumps.

CONCLUSIONS

The WELLNES model is set up for Søndersø waterworks and the contaminated site Værløse air field. The model performs well in both the calibration and the validation period. It simulates the rapid changes in water levels in the wells, when the pump in the well itself or other pumps in the well field are turned on and off. It predicts the total abstraction of water in the calibration period within 5% of the observed value. Søndersø East performs better than Søndersø West. The total energy consumption is predicted within 0.3% of the observed energy consumption for Søndersø East and within 1.8% for Søndersø West.

Multi-objective optimization is applied to improve the management of Søndersø waterworks. The objectives are to minimize the specific energy, E_{spe}, of the waterworks and to maximize the head differences of three pairs of piezometric head observations, H, located between the well fields and the contaminated site. The constraint is to provide a certain amount of water during the period of optimization, and the decision variables are the status of the 11 pumps, which can be turned on or off. Three different optimization scenarios with different population sizes ($\lambda = 16, 20, 26$) are performed. All scenarios show good convergence to the benchmark solution with *HV* between 0.85 and 0.99, and the number of model evaluations are about 10% of all possible solutions.

The results are compared with the simulated historical case, and both objectives can be improved by choosing a solution on the Pareto front. It would, for example, be possible to save 0.006 kWh/m^3 or 4% compared with the simulated historical case and still have the same or slightly better protection against contamination.

This study provides the decision-makers with a powerful management tool. From the Pareto front they can choose one of the optimal solutions, taking into account the advantages and disadvantages of the chosen solution.

ACKNOWLEDGEMENTS

REFERENCES

Bleuler, S., Laumanns, M., Thiele, L. & Zitzler, E. 2003 Pisa – a platform and programming language independent interface for search algorithms. ETH Zürich, Computer Engineering and Networks Laboratory. Available from: www.tik.ee.ethz.ch/sop/pisa/.

Christensen, S. & Hansen, O. 1990 Optimering af indvinding på større kildepladser. *Vandteknik.* **5**, 203–209.

Deb, K. 2001 *Multi-Objective Optimization Using Evolutionary Algorithms*. Wiley, Chichester, UK.

Farmani, R., Savic, D. & Walters, G. 2005 Evolutionary multi-objective optimization in water distribution network design. *Eng. Optim.* **37**(2), 167–183.

Fowler, K. R., Kelley, C. T., Miller, C. T., Kees, C. E., Darwin, R. W., Reese, J. P., Farthing, M. W. & Reed, M. S. 2004 Solution of a well-field design problem with implicit filtering. *Optim. Eng.* **5**(2), 207–234.

Fowler, K. R., Reese, J. P., Kees, C. E., Dennis Jr., J. E., Kelley, C. T., Miller, C. T., Audet, C., Booker, A. J., Couture, G., Darwin, R. W., Farthing, M. W., Finkel, D. E., Gablonsky, J. M., Gray, G. & Kolda, T. G. 2008 Comparison of derivative-free optimization methods for groundwater supply and hydraulic

capture community problems. *Adv. Water Resour.* **31**(5), 743–757.

Graham, D. & Butts, M. 2006 Flexible, integrated watershed modelling with MIKE SHE. In: *Watershed Models* (V. P. Singh & D. K. Frevert, eds). CRC Press, Florida, USA, pp. 245–272.

Gregersen, J. B., Gijsbers, P. J. A. & Westen, S. J. P. 2007 OpenMI: Open modelling interface. *J. Hydroinform.* **9**(3), 175–191.

Halford, K. J. & Hanson, R. T. 2002 *User Guide for the Drawdown-Limited, Multi-Node Well (mnw) Package for the U.S. Geological Survey's Modular Three-Dimensional Finite-Difference Ground-Water Flow Model, Versions Modflow-96 and Modflow-2000*. Technical Report 02-293, US Geological Survey, pp. 4–12.

Knowles, J., Thiele, L. & Zitzler, E. 2006 A *Tutorial on the Performance Assessment of Stochastic Multiobjective Optimizers*. Technical Report 214, Computer Engineering and Networks Laboratory (TIK), ETH Zurich, Switzerland.

Kollat, J. & Reed, P. 2006 Comparing state-of-the-art evolutionary multi-objective algorithms for long-term groundwater monitoring design. *Adv. Water Resour.* **29**, 792–807.

Konikow, L. F., Hornberger, G. Z., Halford, K. J. & Hanson, R. T. 2009 *Revised Multi-Node Well (mnw2) Package for Modflow Ground-Water Flow Model*. Technical Report 6–A30, U.S. Geological Survey, pp. 3–8.

Kürstein, J., Andersen, J. A. & Mahrt, J. 2009 *Sjællandsmodellen – et integreret modelværktøj for det hydrologiske vandkredsløb*. Technical Report, Miljøcenter Roskilde, Chapter 5, pp. 21–41.

Lopez-Ibanez, M., Prasad, D. & Paechter, B. 2008 Ant colony optimization for optimal control of pumps in water distribution networks. *J. Water Resour. Plan. Manage.* **134**(4), 337–346.

Madsen, H., Refsgaard, A. & Falk, A. 2009 Energy optimization of well fields. *Ground Water* **47**(6), 766–771.

Mayer, A., Kelley, C. & Miller, C. 2002 Optimal design for problems involving flow and transport phenomena in saturated subsurface systems. *Adv. Water Res.* **25**, 1233–1256.

Nicklow, J., Reed, P., Savic, D., Dessalegne, T., Harrell, L., Chan-Hilton, A., Karamouz, M., Minsker, B., Ostfeld, A., Singh, A. & Zechman, E. 2010 State of the art for genetic algorithms and beyond in water resources planning and management. *J. Water Resour. Plan. Manage.–ASCE.* **136**, 412–432.

Refsgaard, A., Sidenius, S., Baggerman, P., Madsen, H., Falk, A. K. & Saabøll, H. 2009 *Energibesparelse på kildepladsniveau*. Danva f&u rapport nr. 16, chapter 2, DANVA.

Rossman, L. A. 2000 *Epanet 2 Users Manual*. Technical Report EPA/600/R-00/057, chapters 2–9, U.S Environmental Protection Agency. Available from: www.epa.gov/nrmrl/wswrd/dw/epanet.html.

Siegfried, T., Bleuler, S., Laumanns, M., Zitzler, E. & Wolfgang, K. 2009 Multiobjective groundwater management using evolutionary algorithms. *IEEE Trans. Evol. Comput.* **13**, 229–242.

Siegfried, T. & Kinzelbach, W. 2006 A multiobjective discrete stochastic optimization approach to shared aquifer management: Methodology and application. *Water Resour. Res.* **42**, 1–15.

Thorling, L. 2009 *Grundvandsovervågning 2009 – status og udvikling 1989–2008*. Technical Report chapter 8, De Nationale Geologiske Undersøgelser for Danmark og Grønland – GEUS.

Tsai, F., Katiyar, V., Toy, D. & Goff, R. 2009 Conjunctive management of large-scale pressurized water distribution and groundwater systems in semi-arid area with parallel genetic algorithm. *Water Resour. Manage.* **23**(8), 1497–1517.

van Zyl, J., Savic, D. & Walters, G. 2004 Operational optimization of water distribution systems using a hybrid genetic algorithm. *J. Water Resour. Plan. Manage.–ASCE.* **130**(2), 160–170.

Zitzler, E., Laumanns, M. & Thiele, L. 2002 *Spea2: Improving the Strength Pareto Evolutionary Algorithm*. Technical Report 103, Computer Engineering and Networks Laboratory (TIK), Swiss Federal Institute of Technology (ETH) Zurich, Gloriastrasse 35, CH-8092 Zurich, Switzerland. Available from: www.tik.ee.ethz.ch/pisa/.